HHS Public Access

Author manuscript

Magn Reson Med. Author manuscript; available in PMC 2017 May 01.

Published in final edited form as:

Magn Reson Med. 2016 May ; 75(5): 2078–2085. doi:10.1002/mrm.25799.

Accelerating Magnetic Resonance Fingerprinting (MRF) using t-Blipped Simultaneous Multi-Slice (SMS) acquisition

Huihui Ye[1,2,†], **Dan Ma**[3,†], **Yun Jiang**[3], **Stephen F. Cauley**[2,4], **Yiping Du**[1], **Lawrence L. Wald**[2,4,5], **Mark A. Griswold**[3,6], and **Kawin Setsompop**[2,4]

[1]Collaborative Innovation Center for Brain Science and the Key Laboratory for Biomedical Engineering of Education Ministry of China, Zhejiang University, Hangzhou, Zhejiang, 310027, China

[2]Athinoula A. Martinos Center for Biomedical Imaging, Department of Radiology, Massachusetts General Hospital, Charlestown, Massachusetts, USA

[3]Department of Biomedical Engineering, Case Western Reserve University, 10900 Euclid Avenue, Cleveland, Ohio 44106, USA

[4]Department of Radiology, Harvard Medical School, Boston, Massachusetts, USA

[5]Harvard-MIT Division of Health Sciences and Technology, MIT, Cambridge, Massachusetts, USA

[6]Department of Radiology, Case Western Reserve University and University Hospitals of Cleveland, 11100 Euclid Avenue, Cleveland, Ohio 44106, USA

Abstract

Purpose—We incorporate Simultaneous Multi-Slice (SMS) acquisition into MR Fingerprinting (MRF) to accelerate the MRF acquisition.

Methods—The t-Blipped SMS-MRF method is achieved by adding a G_z blip before each data acquisition window and balancing it with a G_z blip of opposing polarity at the end of each TR. Thus the signal from different simultaneously excited slices are encoded with different phases without disturbing the signal evolution. Further, by varying the G_z blip area and/or polarity as a function of TR, the slices' differential phase can also be made to vary as a function of time. For reconstruction of t-Blipped SMS-MRF data, we demonstrate a combined slice-direction SENSE and modified dictionary matching method.

Results—In Monte Carlo simulation, the parameter mapping from Multi-band factor (MB)=2 t-Blipped SMS-MRF shows good accuracy and precision when compared to results from *reference* conventional MRF data with concordance correlation coefficients (CCC) of 0.96 for T_1 estimates and 0.90 for T_2 estimates. For *in vivo* experiments, T_1 and T_2 maps from MB=2 t-Blipped SMS-MRF have a high agreement with ones from conventional MRF.

Conclusions—The MB=2 t-Blipped SMS-MRF acquisition/reconstruction method has been demonstrated and validated to provide more rapid parameter mapping in the MRF framework.

Corresponding Author: Kawin Setsompop, 149 13th Street. Room 2301, Charlestown, MA, 02129, USA, kawin@nmr.mgh.harvard.edu.
†These authors contributed equally to this work.

Keywords

MR fingerprinting (MRF); Simultaneous multi-slice (SMS); t-Blipped SMS-MRF

INTRODUCTION

Magnetic resonance fingerprinting (MRF) (1) is a relatively recently introduced approach to MR image reconstruction. It uses the generation of temporally and spatially incoherent signal evolutions, or fingerprints, for different tissue types through continuous variation of the acquisition parameters, such as the flip angle (FA), RF phase, TR and sampling pattern. A pattern matching algorithm matchs the fingerprints to a predefined dictionary of predicted signal evolution patterns. The MR parameter maps, such as T_1, T_2, off-resonance and proton density (M_0), are estimated from the best signal matching. Because of the incoherent sampling and the nature of a matching procedure based on preexisting knowledge, MRF has been shown to be less sensitive to errors even in highly undersampled measurements with severe aliasing artifacts.

To enable accurate MR parameters estimation, for each imaging slice, 1000–3000 imaging time points are acquired with repetition time (TR) that is typically about 10 milliseconds, which results in an acquisition time of 10–30 seconds per imaging slice. To create high-resolution volumetric parameter maps of the brain with e.g. 1mm slice thickness, approximately 120 imaging slices must be acquired, resulting in a total acquisition of 20–60 minutes. This long measurement time could hamper wide clinical usage of MRF acquisition.

In this study, we propose to use the Simultaneous Multi-Slice (SMS) imaging technique to accelerate 2D MRF acquisition (SMS-MRF). The SMS technique (2,3) applies multiband (MB) composite RF pulses with a slice-selective gradient to simultaneously excite multiple slice planes. SMS acquisition with parallel imaging reconstruction (4,5) has been improved with the Controlled Aliasing In Parallel Imaging Results In Higher Acceleration (CAIPIRINHA) concept applied to gradient echo imaging with RF phase modulation (6), and adapted in radial imaging with conjugate gradient reconstruction (7). Further, CAIPIRINHA has been successfully implemented in echo planar imaging for functional and diffusion imaging (8–11), where the ‘Blipped-CAIPI’ method provides significant improvement in acceleration performance (10). However, the use of SMS and CAIPIRINHA techniques has not been investigated in MRF. While both the previous methods provide controlled aliasing differences between the simultaneously excited slices in the spatial domain, here, we propose t-Blipped SMS-MRF method with the use of additional G_z blip encodings to provide phase modulation between the signals of simultaneously acquired slices and thus create controlled-aliasing in the time-axis. The combination of slice-direction SENSE (4,12) reconstruction and modified off resonance map smoothness-forced dictionary matching is then proposed for the reconstruction of this data to provide quantitative parameters estimates for the simultaneously acquired slices. We demonstrated that t-Blipped SMS-MRF is able to simultaneously quantify four parameters (T_1, T_2, off-resonance and M_0) from two slices (MB = 2) with no additional time added to the measurement.

METHODS

t-Blipped SMS-MRF Sequence

MRF (1) can be used to acquire multiple parameter maps by matching a long train of highly undersampled images, e.g. from spiral acquisition with up to 48X undersampling, pixel by pixel to a pre-calculated dictionary template. The use of different spiral interleaves for acquisitions at different TRs provides incoherent aliasing as a function of time to enable this matching to work well for such a highly undersampled dataset. Along a similar line, with t-Blipped SMS-MRF, we aim to introduce slice-specific phase terms across time. The t-Blipped method is achieved by adding a G_z blip before each data acquisition window and balancing it after the acquisition window in each TR. With such addition, the signals from different simultaneously excited slices will be encoded with different phases depending on their slice positions. In the UNFOLD method (13), voxels are in-plane aliased but the aliasing is phased modulated across time which helps control aliasing. In a similar way for t-Blipped method, with the additional added phase differences on the slices, voxels after separation are still with residual aliasing but the aliasing from the other slice is phase modulated along time axis. The overall t-Blipped SMS-MRF sequence is shown in Fig. 1. Similar to the MRF sequence, the t-Blipped SMS-MRF sequence uses a varying RF and TR train played on an IR-TrueFISP based sequence, with the single band RF pulse replaced with multi-band VERSEd (14) pulse and small G_z gradient blips of area A_{blip} and $-A_{blip}$ added before and after the data acquisition window respectively. The added G_z gradient blip will introduce a phase difference for simultaneously excited slices equals to $2\pi\gamma A_{blip}D$ where γ is the gyromagnetic ratio and D is distance between the simultaneously excited slices. For the MB = 2 case of t-Blipped SMS-MRF that will be used in this work, G_z blips are applied to create π phase difference between two simultaneously excited slices for the even TRs, while no G_z blips are applied for the odd TRs. If desired, the blips can be added to the slice refocus/prefocus gradient to save time.

Quantitative Parameter Estimate Reconstruction

In this work, standard MRF reconstruction method for quantitative parameters estimate, as outlined in (1), is used on conventional MRF data that is acquired for comparison. For each TR, the signal from each receiver coil is first reconstructed using NUFFT-based gridding method (15) and then combined using coil sensitivities estimated from the adaptive combination method (16) applied to the average images across the initial 100 reconstructed time points (TRs). For each voxel, the reconstructed time-series is then compared to a pre-computed MRF dictionary. This MRF dictionary was created from the Bloch equations using 1966 combinations of T_1 and T_2 values, each of which are considered against 137 possible off resonance values. Varying step sizes were used to cover T_1, T_2 and off resonance values in the ranges of [100, 5000], [20, 1900], and [−300, 290] respectively. For each voxel, quantitative parameter estimates are obtained from the dictionary element with the highest normalized correlation to the time-series signal of that voxel.

For t-Blipped SMS-MRF, the above reconstruction procedure was modified to enable estimation of quantitative parameters for simultaneously acquired slices. Fig. 2(a) shows the overall reconstruction pipeline for t-Blipped SMS-MRF. First, gridding reconstruction is

applied to the slice-collapsed data. Slice-direction SENSE reconstruction (4,12) is then applied using coil sensitivity estimates obtained from the slice-collapsed SMS-MRF data via a modified adaptive combination procedure (see below). Since the voxel aliasing in the slice and the in-plane directions are coupled the application of slice-direction SENSE would not provide a clean separation between the two imaging slices. Nonetheless, slice-direction SENSE provides partial separation and phase modulation from the G_z blips further decouples the signal in order to provide accurate quantitative parameter estimation. Note that phase demodulation for the separate signals from simultaneous excited slices is applied before dictionary matching. After an initial dictionary matching, this reconstruction pipeline provides good quantitative estimates in most areas of the imaging slices, but can perform poorly at a few speckled voxels where large errors in the off-resonance estimate are observed. To further improve the result, prior knowledge of slowly varying off resonance map is used. Here, the estimated off-resonance map is median filtered [5 voxel × 5 voxel] and voxels with a large change in off-resonance of more than 10Hz are recorded. For these voxels, a secondary dictionary-matching step is performed, where the off-resonance value from the median filtered off-resonance map is used as an anchor to improve the estimated values for T_1, T_2 and M_0.

As mentioned above a modified adaptive combination method is used to obtain coil sensitivity estimates from the t-Blipped SMS-MRF data. For the MB=2 case employed in this work, the signal phase of slice one located at the isocenter is not modulated, whereas the signal phase of slice two contains a 0-π alternating phase modulation as a function of TR. To estimate the coil sensitivity for slice one, the data from the first 400 time points are directly summed. With this summation, the 0-π phase modulation in slice two will cause the signal from adjacent time points in this slice to approximately cancel out, while for slice 1, the signal should sum constructively to average out the image contrast of different time points to provide smooth coil sensitivities (7). To estimate the coil sensitivity for slice two, the data from the first 400 time points are phase demodulated by 0-π and then summed. Here, the signal from slice two should sum coherently while the signal from slice one should cancel. Examples of the coil sensitivity maps from coils 5 and 9 obtained from the procedure are shown in Fig. 2(b). The similarity of these maps with those obtained from single-slice MRF can be clearly observed.

Acquisition

To validate the t-Blipped SMS-MRF method, data were acquired *in vivo* from a single healthy volunteer with institutionally approved protocol consent, using a 3T Siemens Skyra a standard Siemens 16-channel head array coil (20 channel head-neck coil with the 4 neck channels off). The two datasets acquired were i) two slices of conventional MRF data at a distance of 40 mm apart at an acquisition time of 10s/slice and ii) t-Blipped SMS-MRF data with MB =2, acquiring the same exact two slices simultaneously, resulting in an improved acquisition rate of 5s/slice. As described in (1), an IR-trueFISP based sequence with varying FA and TR was used to acquire data at 1000 time points for both of these datasets. Both conventional and SMS-MRF experiments were performed with a Perlin noise shaped TR time distribution ranging from 8.2ms to 10.56ms and the flip angle time serial uses a noise-added sinusoidal shape and is restricted to be within 0° to 60° to ensure good quality slice

profiles. The inversion pulse is non-selective and adiabatic, and the excitation RF in each TR is VERSEd (14) with a slice thickness of 5mm. At each time-point or TR, one of the 48 variable density spiral interleaves (48X) was used to read out the signal, with a designed square FOV of 300mm and square matrix size of 128. After the inversion, data for 48 spiral interleaves are acquired in a sequential manner repeatedly until a total of 1000 time points (TRs) are created per inversion pulse. The use of non-selective inversion pulse in this sequence should not be detrimental to multi-slice (whole brain) acquisition. Following each non-selective inversion pulse, data is acquired using slice selective excitation for a period of ~10s (1000 TRs), so there should be adequate time for the out of slice's gray and white matter magnetization to recover prior to the next inversion pulse and acquisition. The point spread function (PSF) from 2 selected spiral interleaves are shown in Fig, 1(c). To introduce a global phase shift to the time point for every other slice in t-Blipped SMS-MRF scan, for the even TRs, G_z blips were applied to create π phase difference between the two simultaneously excited slices. For the odd TRs, no G_z blips were applied.

Evaluation and Comparison

We evaluated the benefits of the MB=2 t-Blipped SMS-MRF method by comparing the following acquisition alternatives: i) conventional MRF results obtained from 10s/slice scan (20s total acquisition time), ii) conventional MRF results obtained from shorter time-series (resulting in 5s/slice scan that therefore matched the 10s total acquisition of the MB=2 SMS-MRF acquisition, and iii) MB=2 t-Blipped SMS-MRF results obtained from a 5s/slice scan (10s total acquisition time).

To investigate the accuracy and precision of MB=2 t-Blipped SMS-MRF, simulations using a bootstrapped Monte Carlo method (17) on all the three aforementioned cases were conducted. In addition, simulation of MB=2 non-Blipped SMS-MRF case is also conducted and compared. In conventional MRF cases, noise was added to the acquired data by drawing from the noise distribution defined by the measured noise–covariance matrix. The added noise level was set to be the same as the noise level of the acquired data thus doubling the total noise in single slice case. Sixty sets of two conventional MRF data were generated and reconstructed using the standard MRF reconstruction method. For the MB=2 t-Blipped SMS-MRF case, comparable data were simulated by summing the acquired single-slice MRF data, thus doubling the noise; with an added 0-π phase modulation to the second slice data prior to the summation. For the MB=2 non-Blipped SMS-MRF case, comparable data were simulated by summing the acquired single-slice MRF data. Analogous to the conventional MRF case, noise was added to this synthesized t-Blipped and non-Blipped SMS-MRF data (total triple noise) and 60 datasets were generated and reconstructed using the method outlined above. For reference, 10s/slice conventional MRF data without additional noise were reconstructed for comparison. Three different metrics were adopted to evaluate the simulation results: i) Differences in the T_1 and T_2 mean maps of the 3 cases against the reference maps were computed to show the average bias in the three cases. In addition, averages of the T_1 and T_2 difference maps were also calculated to indicate the total bias in each case, ii) the concordance correlation coefficients (CCC) in the brain area between average simulation values and reference results were calculated (18), and iii) 100 random pixels in each slice were picked, and correlation plots between the average results

and reference results was measured. Here, the along standard deviation value was used to indicate the confidence intervals at each point.

In addition to Monte Carlo simulation, reconstructions of *in vivo* data for the three acquisition cases (without additional added noise) were performed and the resulting T_1, T_2, off resonance and M_0 maps were compared.

RESULTS

Fig. 3 shows of the average T_1 and T_2 difference maps based on the Monte Carlo simulation of the four cases, when compared to results from the 10s/slice reference conventional MRF case without added noise. As expected, the 10s/slice conventional MRF case shows the smallest difference, while the 5s/slice conventional MRF case shows the largest. The 5s/slice MB=2 t-Blipped SMS-MRF case falls between the two conventional MRF cases, pointing to an improvement in acquisition time efficiency with this slice accelerated acquisition. The mean T_1 and T_2 differences in the brain area, where the reference T_2 value is within a realistic range for gray and white matter (below 300ms), were also calculated. For the 10s/slice conventional MRF case, the mean differences of T_1 and T_2 were 4.5ms and 0.7ms. For the 5s/slice conventional MRF these were 87.7ms and 23.3ms, and for the 5s/slice MB=2 t-Blipped case these were 75.4ms 8.0ms. The 5s/slice MB=2 non-Blipped SMS-MRF case shows similar bias level with the t-Blipped case while shows obvious boundary artefact which is not seen in t-Blipped case.

Fig. 4 shows the correlation plots of mean +/− standard deviation of T_1 and T_2 values from 100 randomly picked voxels (marked in T1 map in Fig. 3 with green circles) from the Monte Carlo simulations. Here, the four acquisition alternatives are compared to the 10s/slice reference conventional MRF case without added noise. The CCCs of the brain area are also reported on the plots. From these results, it can be observed that the consistency of T_1 estimates is better than T_2 estimates in all three cases, with the 5s/slice conventional MRF case showing the largest bias and worst stability in both T_1 and T_2 estimates, the 10s/slice conventional MRF case providing the best estimates, and t-Blipped case shows better consistency than non-Blipped case. In all cases, the standard deviation values, indicated as error bars on the plots, are much smaller in comparison to the bias of these estimates.

Fig. 5 shows the *in vivo* results from the three acquisition cases, with results of MB=2 shown for both the first and the second dictionary matching (employing smooth off-resonance prior). Overall, the MB=2 acquisition (after the second matching step) provides comparable results to the 10s/slice conventional MRF acquisition, with much better consistency when compared to the 5s/slice conventional MRF case. Specifically, in the 5s/slice conventional MRF results, the parameter maps appear more blurry with large residual ringing artifacts (areas designated by gray boxes). Additionally, as predicted by the simulation, the T_2 values in this case appear markedly lower. This is highlighted by the area within the green zoomed box. Significant speckle artifact can also be observed. The MB=2 results provides a significant improvement when compared to this acquisition of identical duration. In addition, after the second matching step for MB=2, the speckled artifacts in the T_1, T_2 and M_0 maps have been successfully removed (an example instance is shown in the

zoomed blue boxes). The results of MB=2 are generally in accordance with that of the 10s/slice conventional MRF case as predicted by simulation. Nonetheless, a small deviation can be observed in a somewhat lowered T_2 value of the upper imaging slice. We note that the off-resonance maps obtained from MB=2 acquisition are different to that from the conventional MRF cases. This is expected since different B_0 shim settings were used, where in the MB=2 acquisition the shim volume is larger to cover the two slices simultaneously.

DISCUSSIONS

In this work, we propose the t-Blipped SMS-MRF acquisition/reconstruction method and demonstrate its capability in accelerating MRF through a MB=2 slice-accelerated acquisition. The method was reliable in simulation and *in vivo* on a healthy volunteer and can be used to provide faster quantitative information of the brain. This acquisition scheme reduces the MRF imaging time per slice by half to 5s, and could facilitate volumetric MRF mapping at high resolution in a clinically relevant time frame.

From the Monte Carlo simulation, it can be observed that with the IR-trueFISP based MRF sequence, T_1 values can be more robustly estimated from a reduced dataset (5s/slice conventional MRF and MB=2 case) with less bias and variant when compare to T_2 value estimates. This indicates that the present MRF sequence setting is more robust for T_1 characterization. In a reduced dataset, speckle artifacts in the parameter maps are also present and the use of prior information of spatially smooth off-resonance has been shown to robustly remove these artifacts in MB=2 reconstruction. We note that such speckle artifacts affect only a small portion of the image voxels and as such the second dictionary matching step should add negligible processing time. Moreover, this proposed method should also be applicable in improving the results for the conventional MRF case. In our experimental comparison of MB=1 and MB=2 acquisitions, different B_0 shim settings were used for the two acquisitions. As expected, this resulted in differences in off resonance maps. Potentially, this difference in shim settings could also affect the robustness of T_1 and T_2 estimates; a topic that applies to MRF in general which still requires further investigation. Nonetheless, we note that in our comparison, the shim differences do not seem to change the T_1 and T_2 values. We note that in an IR-TrueFisp sequence, significant image contrast variations are present during the first 400 time points due to the T_1 recovery process. Nonetheless, the averaging of 400 time points, each with different aliasing, is sufficient in removing this variation in contrast to provide smooth coil sensitivities. We also note that the use of SMS-MRF data to calculate coil sensitivity maps does not incur additional acquisition time but may not be optimal, and other prescan methods can also be explored to potentially improve performance. The spiral trajectory is pre-designed and not adjustable during the scan, so the FOV of the spiral trajectory was purposely designed to be relatively large to cover all possible user cases.

This work demonstrates the ability to accelerate MRF acquisition using SMS-MRF method. The proposed technique utilizes additional G_z blip encoding prior to standard spiral readout to provide differential encoding between slices. By varying the G_z blips area and/or polarity as a function of TR, the phase difference between slices can be made to vary during the SMS-MRF acquisition to create helpful temporal modulation in the slice aliasing effect. In

comparison, using slice-specific RF excitation phase can also provide differential encoding between slices, however, it cannot be easily rewinded after the readout thus cannot at the same time keep the original RF phase cycling pattern. The RF phase cycling pattern is needed to achieve a balanced SSFP sequence with signal maximum for on resonance spins ($\Delta B0=0$). In this work the G_z blips are used to create a simple 0-π phase modulation that was shown to work well for the MB=2 acquisition. We note that the Gz blip-related through-slice dephasing and eddy current effects are insignificant in typical imaging cases, as previously demonstrated in the blipped-CAIPI work (10), where not only one but multiple additional Gz blips are added per readout without significant dephasing and/or eddy current issue. Other patterns of phase modulation will be further explored, compared and optimized. With the proposed method, the gridding procedure only needs to be conducted once for two slices. Additionally, the same dictionary can be used for both slices, which is beneficial for memory consideration because the MRF dictionary used in this work requires 1966×137×1000×4 bytes (~1GB) of memory. Moreover, additional complementary methods to create differential encoding or differences in fingerprints between the simultaneously excited slices will be explored to help achieve higher MB accelerations. Such techniques include the exploration into slice specific flip-angle train in MB excitation, the use of G_z blips during the spiral encoding that has been previously utilized in SMS-spiral for fMRI (5,19), and highly under-sampled volumetric acquisition schemes. Specifically, the use of additional G_z blips during the spiral encoding would improve slice unaliasing and increase achievable slice acceleration factor when combined with the use of specific reconstruction method. As for volumetric acquisitions, it would result a long readout duration or long time series in using single shot acquisition even with a high under-sampling factor. When multi-shot acquisition is used, it would also lengthen the acquisition time and incur shot-to-shot motion effects. In both cases for volumetric acquisitions, some form of additional acceleration will be needed and will be investigated in future work.

Full parallel imaging reconstruction at each time-point (TR) is extremely ill conditioned since the data is highly undersampled in the in-plane direction (up to 48X) with additional aliasing in the slice direction (MB=2). Therefore, the SENSE reconstruction method that has been used in previous SMS works (4,5) which unalias both in-plane and slice direction simultaneously could not be employed here. Rather, in this work, we utilized slice-direction SENSE reconstruction to provide partial unaliasing in the slice direction. This unaliasing procedure is ill formed since, in the SENSE model, the aliasing is coupled in both slice and in-plane directions. Nonetheless, such procedure does improve reconstruction performance. Further investigation into k-space based parallel imaging reconstructions, which enabled separate unaliasing in e.g. the slice direction only, will be investigated. In particular, the combination of GROG (20–22) and slice-GRAPPA (10,23) should provide improved reconstruction that will enable further MB accelerations.

The use of MB factors above 2 (up to MB = 4 or 6) is normally not problematic for conventional sequences when CAIPI slice shift technique is used along with a 32ch brain array (or even the 16ch used here). However, we found that the MRF T_1 and T_2 mapping were severely compromised for MB factors above 2, as can been seen in supporting figure S1. One reason is that, like conventional SMS, the in-plane acceleration and MB acceleration fight each-other in that addition of in-plane acceleration reduces the benefit of

the slice shift. Ultimately, the distance between aliased pixels is dominated by the larger of the two acceleration factors. The 48x undersampled conventional single-slice MRF with 1000 timepoints falls in the category of “heavily in-plane accelerated” and is already a difficult reconstruction problem. For example parallel imaging fails to reconstruct the individual R=48 accelerated time-point images. The parallel imaging (SENSE) is only used in the slice direction and, like conventional SMS, is limited by the interplay between acceleration in the slice and in-plane directions. Another reason is that, the use of t-Blipped method doesn’t introduce slice shift while instead it encodes a specific amount of phase difference between slices in each timepoint. As was previously demonstrated that without the use of CAIPI shift in standard SMS-EPI acquisition, MB-3 acceleration causes a large SNR drop of up to 50% at 3T when 32-channel head array is used (10), MB-3 accelerated MRF will suffer drastic penalty in g-factor noise.

Supplementary Material

Refer to Web version on PubMed Central for supplementary material.

Acknowledgments

This work has been supported through the NIH NIBIB grants R01EB017219, R00EB012107, R01EB017337and P41EB015896, the National Key Basic Research Program of China (2013CB329501) and the National Natural Science Foundation of China (81371518).

References

1. Ma D, Gulani V, Seiberlich N, Liu K, Sunshine JL, Duerk JL, Griswold MA. Magnetic resonance fingerprinting. Nature. 2013; 495(7440):187–192. [PubMed: 23486058]
2. Souza SP, Szumowski J, Dumoulin CL, Plewes DP, Glover G. SIMA: simultaneous multislice acquisition of MR images by Hadamard-encoded excitation. J Comput Assist Tomogr. 1988; 12(6): 1026–30. [PubMed: 3183105]
3. Weaver JB. Simultaneous multislice acquisition of MR images. Magn Reson Med. 1988; 8(3):275–84. [PubMed: 3205156]
4. Larkman DJ, Hajnal JV, Herlihy AH, Coutts GA, Young IR, Ehnholm G. Use of multicoil arrays for separation of signal from multiple slices simultaneously excited. J Magn Reson Imaging. 2001; 13(2):313–317. [PubMed: 11169840]
5. Zahneisen B, Poser BA, Ernst T, Stenger VA. Three-dimensional Fourier encoding of simultaneously excited slices: Generalized acquisition and reconstruction framework. Magn Reson Med. 2014; 71(6):2071–81. [PubMed: 23878075]
6. Breuer FA, Blaimer M, Heidemann RM, Mueller MF, Griswold MA, Jakob PM. Controlled aliasing in parallel imaging results in higher acceleration (CAIPIRINHA) for multi-slice imaging. Magn Reson Med. 2005; 53(3):684–91. [PubMed: 15723404]
7. Yutzy SR, Seiberlich N, Duerk JL, Griswold MA. Improvements in multislice parallel imaging using radial CAIPIRINHA. Magn Reson Med. 2011; 65(6):1630–7. [PubMed: 21287592]
8. Moeller S, Yacoub E, Olman CA, Auerbach E, Strupp J, Harel N, Ugurbil K. Multiband multislice GE-EPI at 7 tesla, with 16-fold acceleration using partial parallel imaging with application to high spatial and temporal whole-brain fMRI. Magn Reson Med. 2010; 63(5):1144–53. [PubMed: 20432285]
9. Nunes, R.; Hajnal, J.; Golay, X.; Larkman, D. Simultaneous slice excitation and reconstruction for single shot EPI. Proc Intl Soc Mag Reson Med; 2006; p. 293
10. Setsompop K, Gagoski BA, Polimeni JR, Witzel T, Wedeen VJ, Wald LL. Blipped-controlled aliasing in parallel imaging for simultaneous multislice echo planar imaging with reduced g-factor penalty. Magn Reson Med. 2012; 67(5):1210–24. [PubMed: 21858868]

11. Feinberg DA, Moeller S, Smith SM, Auerbach E, Ramanna S, Gunther M, Glasser MF, Miller KL, Ugurbil K, Yacoub E. Multiplexed echo planar imaging for sub-second whole brain FMRI and fast diffusion imaging. PLoS One. 2010; 5(12):e15710. [PubMed: 21187930]
12. Pruessmann KP, Weiger M, Scheidegger MB, Boesiger P. SENSE: sensitivity encoding for fast MRI. Magn Reson Med. 1999; 42(5):952–962. [PubMed: 10542355]
13. Madore B, Glover GH, Pelc NJ. Unaliasing by Fourier-Encoding the overlaps using the temporal dimension (UNFOLD), applied to cardiac imaging and fMRI. magnetic resonance in medicine. 1999; 42:16.
14. Conolly S, Nishimura D, Macovski A, Glover G. Variable-rate selective excitation. J Magn Reson. 1988; 78(3):440–458.
15. Fessler JA. On NUFFT-based gridding for non-Cartesian MRI. J Magn Reson. 2007; 188(2):191–5. [PubMed: 17689121]
16. Walsh DO, Gmitro AF, Marcellin MW. Adaptive reconstruction of phased array MR imagery. Magn Reson Med. 2000; 43(5):682–90. [PubMed: 10800033]
17. Riffe, M.; Blaimer, M.; Barkauskas, K.; Duerk, J.; Griswold, M. SNR estimation in fast dynamic imaging using bootstrapped statistics. Proc Intl Soc Mag Reson Med; 2007; p. 1879
18. Lawrence I, Lin K. A concordance correlation coefficient to evaluate reproducibility. Biometrics. 1989:255–268. [PubMed: 2720055]
19. Zahneisen B, Poser BA, Ernst T, Stenger AV. Simultaneous Multi-Slice fMRI using spiral trajectories. NeuroImage. 2014; 92:8–18. [PubMed: 24518259]
20. Seiberlich N, Breuer FA, Blaimer M, Barkauskas K, Jakob PM, Griswold MA. Non-Cartesian data reconstruction using GRAPPA operator gridding (GROG). Magn Reson Med. 2007; 58(6):1257–65. [PubMed: 17969027]
21. Seiberlich N, Breuer F, Heidemann R, Blaimer M, Griswold M, Jakob P. Reconstruction of undersampled non-Cartesian data sets using pseudo-Cartesian GRAPPA in conjunction with GROG. Magn Reson Med. 2008; 59(5):1127–1137. [PubMed: 18429026]
22. Griswold MA, Blaimer M, Breuer F, Heidemann RM, Mueller M, Jakob PM. Parallel magnetic resonance imaging using the GRAPPA operator formalism. Magn Reson Med. 2005; 54(6):1553–6. [PubMed: 16254956]
23. Griswold MA, Jakob PM, Heidemann RM, Nittka M, Jellus V, Wang J, Kiefer B, Haase A. Generalized autocalibrating partially parallel acquisitions (GRAPPA). Magn Reson Med. 2002; 47(6):1202–10. [PubMed: 12111967]

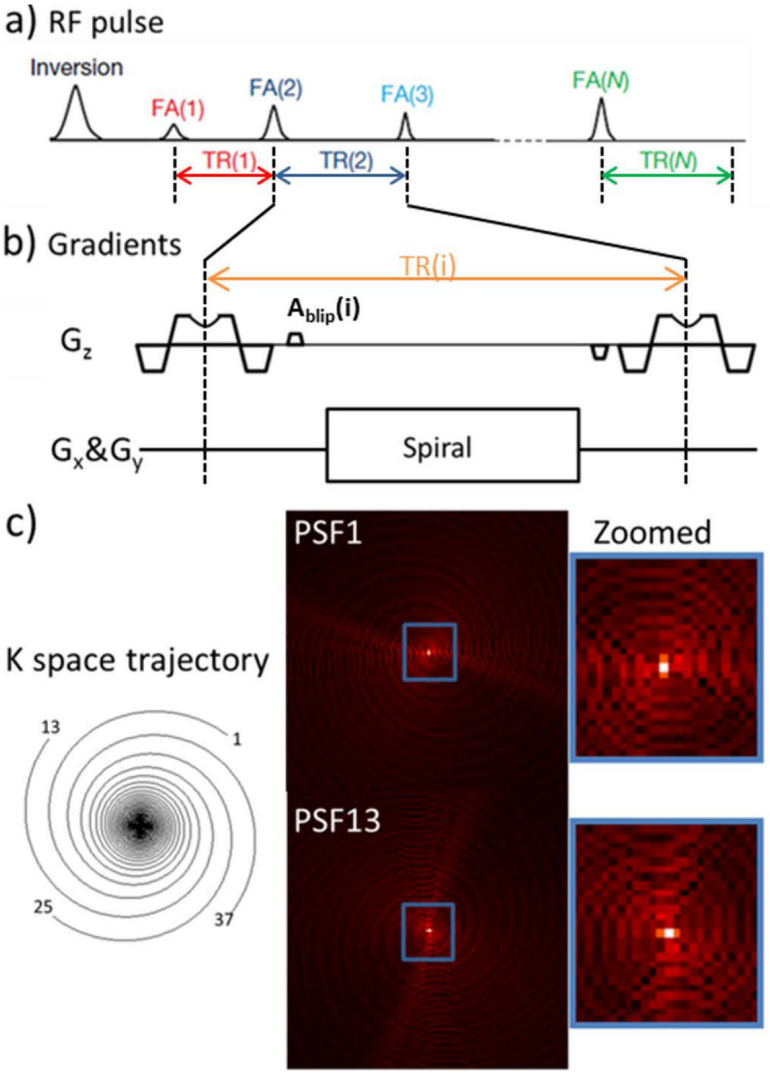

Fig. 1.

Scheme of the proposed t-Blipped SMS-MRF acquisition for an acquisition with MB=2. (a) the RF pulse train used in the IR-trueFISP sequence on which the MRF acquisition is based. The inversion pulse is non-selective but each subsequent RF pulse is a multi-band RF which simultaneous excites 2 slices. (b) Detail of the slice selection with VERSE during the RF and the t-Blipped method of imposing phase shifts on the different slice positions of the excited slices in one TR. Here in this MB=2 acquisition, A_{blip} is the area added to the normal prephasing lobe to provide a phase difference of pi to simultaneously excited slices in the even numbered TRs. This blip area is rewinded after the readout. No blip is added on the odd numbered TRs, creating a zero phase difference between the slices. Signal is read out using spiral trajectory.(c) One of 48 highly under-sampled (48X) variable density spiral interleaves is used in each TR, and corresponding ring-like PSFs plotted.

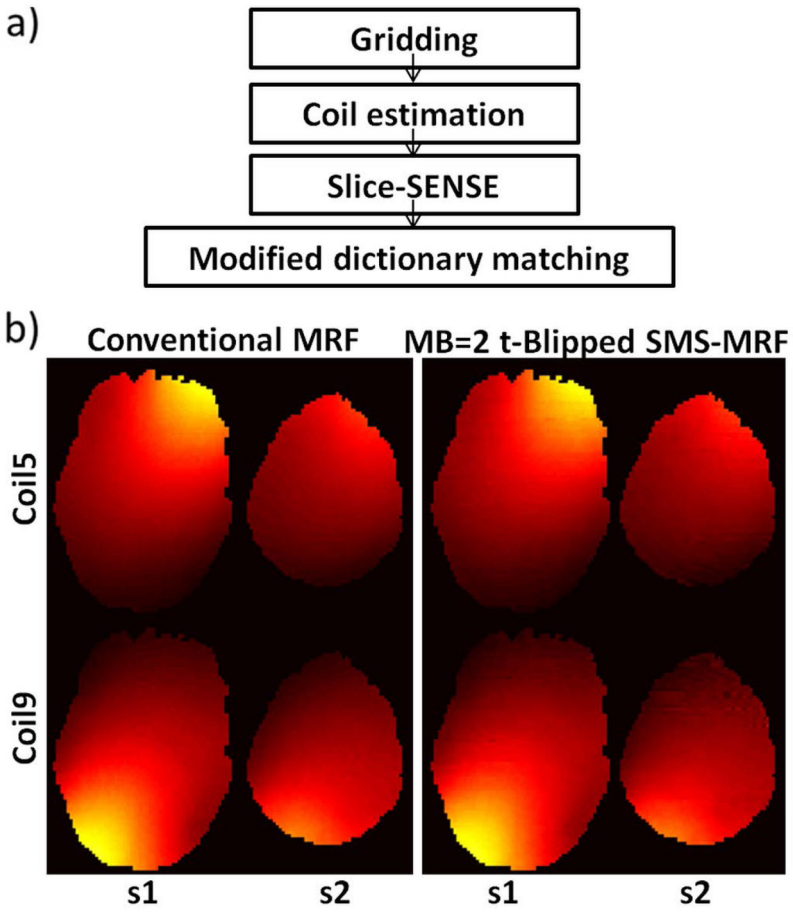

Fig. 2.

(a) Flow chart of t-Blipped SMS-MRF data reconstruction with slice-direction sense method. Images from each time point in each channel were reconstructed separately using non-uniform Fourier transform (NUFFT). Sensitivity map for each slice is estimated using adaptive combination method using the average image across the initial 400 reconstructed time points. Slice sense reconstruction is then applied to obtain the single slice image series. For each slice, dictionary matching method is used pixel-wise to determine the value for the parameters (T_1, T_2, off-resonance and M_0). Prior knowledge of smooth off resonance map is adapted to refine the matched off resonance map, and the other maps are updated with this known smooth off resonance map after a second dictionary matching. (b) Coil sensitivity maps (coil 5&9) calculated from conventional MRF data and MB=2 t-Blipped SMS-MRF data.

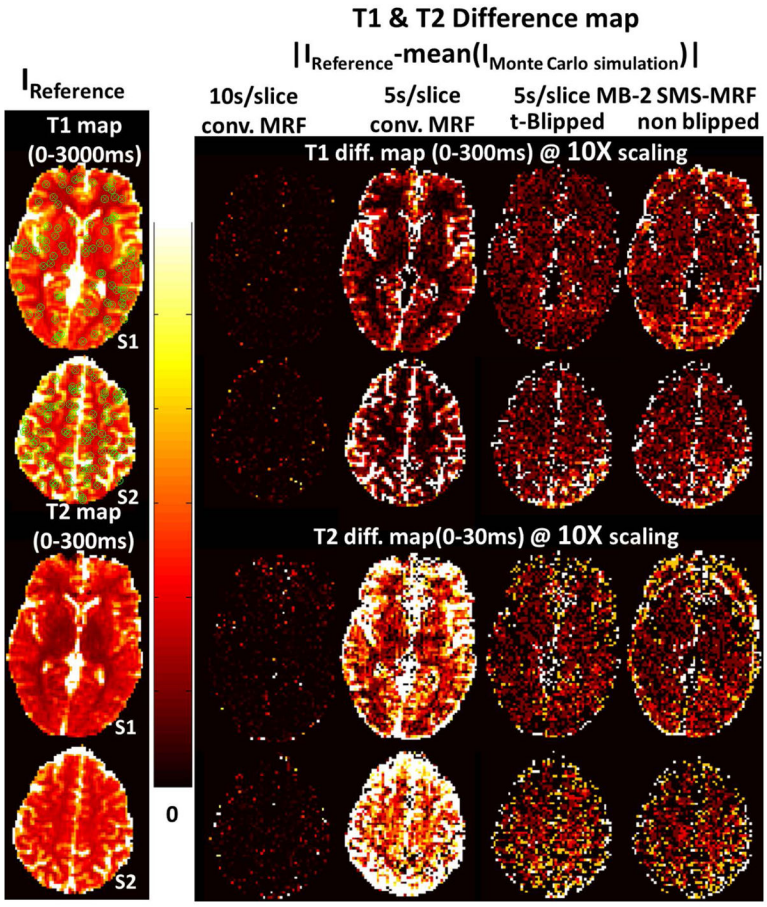

Fig. 3.

Monte Carlo simulation results (two slices): First column shows the reference T1 and T2 map ($I_{Reference}$) from 10s conventional MRF. The other columns shows the absolute T1 and T2 difference between mean Monte Carlo simulation results and reference maps. The four cases are: 10s/slice conventional MRF, 5s/slice conventional MRF case, 5s/slice MB=2 t-Blipped SMS-MRF, and 5s/slice MB=2 non-Blipped SMS-MRF. The color bar limits are listed on each figure.

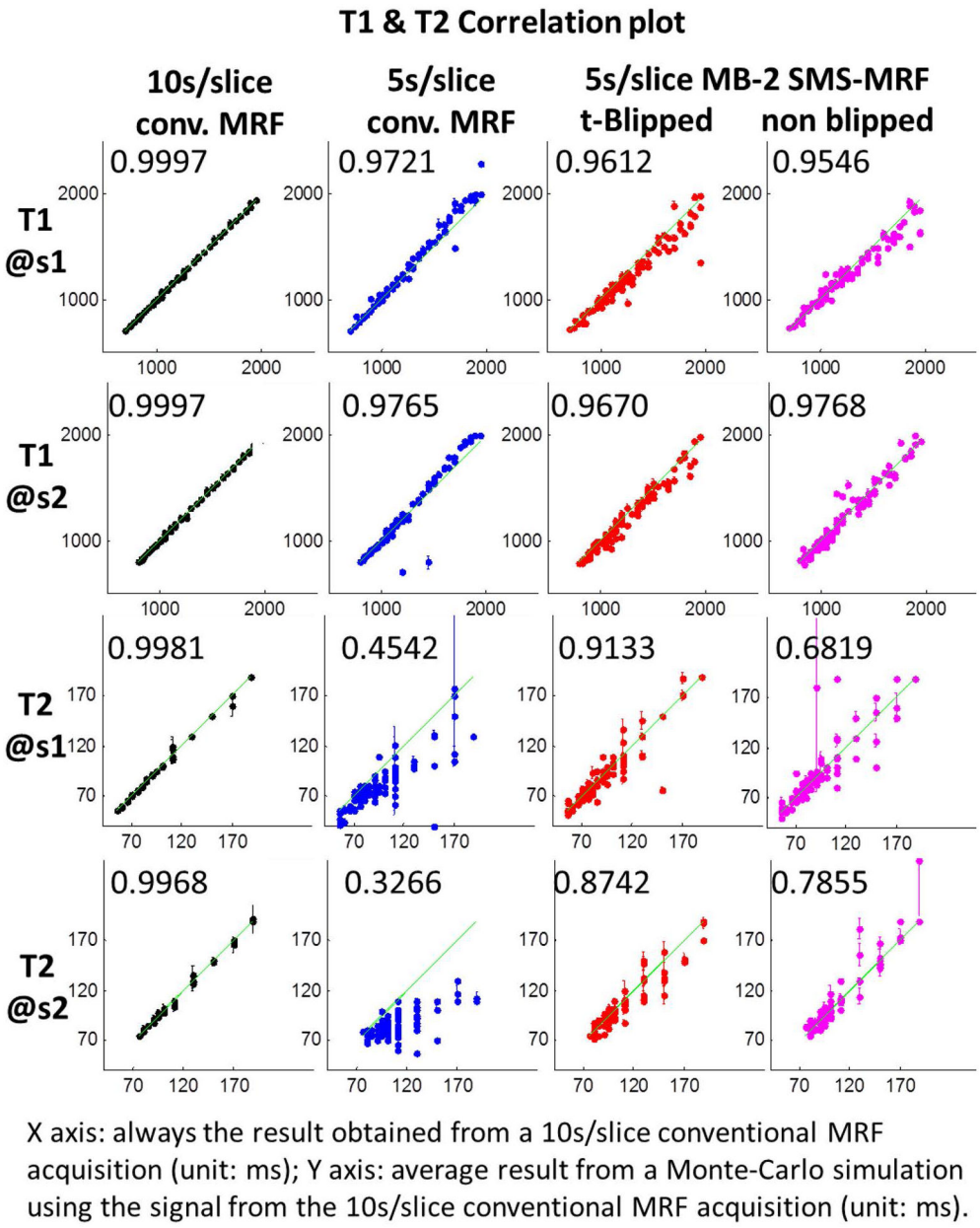

Fig. 4.

Correlation plots between mean Monte Carlo simulation results and reference map from randomly selected 100 points in each slice (marked in T1 map in Fig. 3 with green circles) with error bar (standard deviation value) added in each point to indict the confidence interval. Labeled in each plot is the CCCs calculated in the brain area.

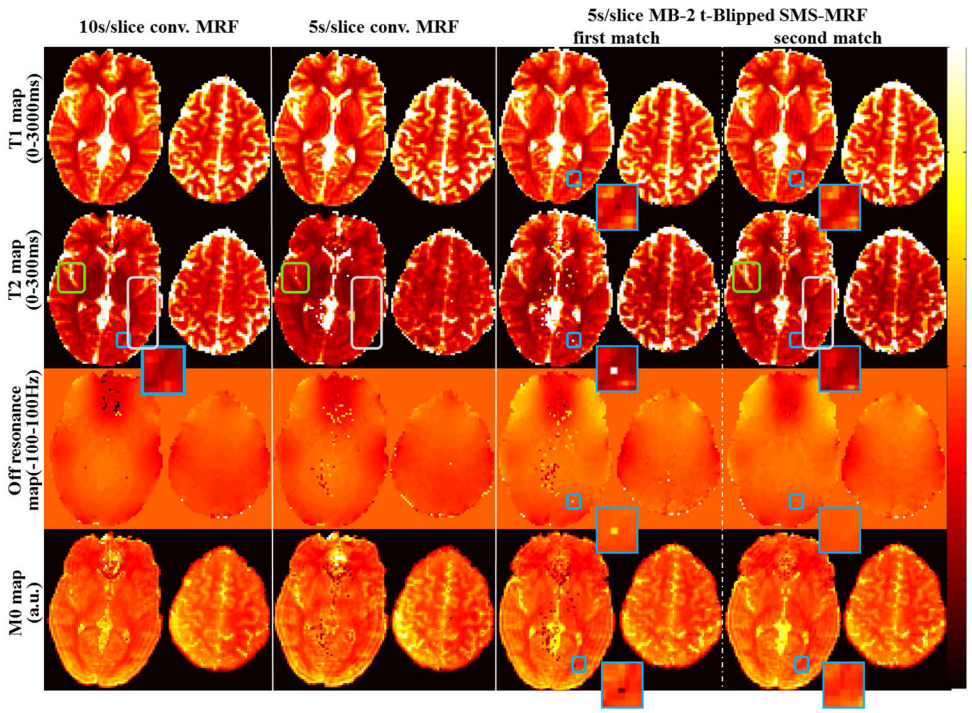

Fig. 5.

In vivo T_1, T_2, off resonance and M_0 maps from four experimental different cases: i) 10s/slice conventional MRF, ii) 5s/slice conventional MRF, iii) 10s MB=2 t-Blipped SMS-MRF after first match, and iv) 10s MB=2 SMS-MRF after second match. The color bar limits for each type of map are listed on the left.